Original Paper

phys. stat. sol. (a) **202**, No. 14, 2591–2597 (2005) / **DOI** 10.1002/pssa.200562029

Dark exciton decay dynamics of a semiconductor quantum dot

Paul A. Dalgarno[1], **Jason M. Smith**[**, 1], **Brian D. Gerardot**[1], **Alexander O. Govorov**[2], **Khaled Karrai**[3], **Pierre M. Petroff**[4], and **Richard J. Warburton**[*, 1]

[1] School of Engineering and Physical Sciences, Heriot-Watt University, Edinburgh EH14 4AS, UK
[2] Department of Physics and Astronomy, Ohio University, Athens, Ohio, USA
[3] Center for NanoScience and Department für Physik, Ludwig-Maximilians-Universität, 80539 München, Germany
[4] Materials Department, University of California, Santa Barbara, California 93106, USA

Received 5 July 2005, revised 16 July 2005, accepted 23 September 2005
Published online 4 November 2005

PACS 71.35.–y, 73.21.La, 78.67.Hc

We report measurements of the exciton decay dynamics of a single self-assembled quantum dot following non-resonant excitation. The singly charged exciton, the trion, exhibits a simple one component exponential decay corresponding to radiative recombination. Conversely, the neutral exciton exhibits a two component exponential decay. We argue that the secondary component arises from dark exciton creation and subsequent conversion to a bright exciton through a spin flip. The spin flip time is a strong function of the bias applied between a Fermi reservoir close to the dot and a Schottky gate electrode as a result of a Kondo-like spin swap process.

© 2005 WILEY-VCH Verlag GmbH & Co. KGaA, Weinheim

1 Introduction

The neutral exciton in a self-assembled quantum dot has a pronounced fine structure [1]. The bright exciton states with spin 1 lie a few hundred μeV above the dark states with spin 2 as a consequence of the spin-dependent electron–hole exchange interaction. Furthermore, the anisotropic part of this interaction splits the bright states by tens of μeV. Conversely, recent experiments have demonstrated that the singly charged exciton, the trion, has no fine structure because the electron spin is zero [1–4]. We report here the consequences of the fine structure on the decay dynamics of an exciton following non-resonant excitation.

2 Exciton decay dynamics

The InGaAs quantum dots were fabricated by MBE exploiting a strain-driven self-assembly process. The dots are separated by a tunneling barrier from a Fermi sea of electrons. The tunnel barrier consists of 25 nm undoped GaAs and the Fermi sea is a GaAs n^+ layer. The dots are 150 nm below the surface of the heterostructure onto which a NiCr gate is evaporated. The gate forms a Schottky contact and by means of an applied voltage, the quantum dot energy levels can be tuned relative to the Fermi energy of the Fermi sea. The experiment involves measuring the photoluminescence (PL) from a single quantum dot at 5 K. The PL exhibits a pronounced Coulomb blockade, as shown in Fig. 1. At large negative voltages the dot does not emit; at –0.42 V, the neutral exciton (X^0) emerges, and then at –0.24 V the X^0 is

* Corresponding author: e-mail: R.J.Warburton@hw.ac.uk, Phone: +44 131 4518096, Fax: +44 131 4513136
** Present address: Department of Materials, University of Oxford, Parks Road, Oxford OX1 3PH, UK

WILEY InterScience® DISCOVER SOMETHING GREAT

© 2005 WILEY-VCH Verlag GmbH & Co. KGaA, Weinheim

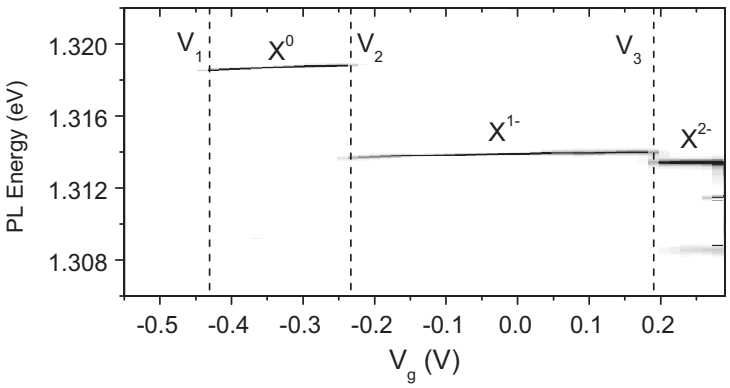

Fig. 1 Gray-scale plot of the photoluminescence (PL) from a single quantum dot versus gate voltage V_g at 5 K. White corresponds to 0 counts, black to 1000 counts. The neutral exciton, X^0, exists between $V_g = V_1$ and $V_g = V_2$. At $V_g = V_2$, the X^0 emission is replaced by emission from the singly-charged exciton, the trion, X^{1-}. At $V_g = V_3$, the X^{1-} is replaced by the X^{2-}.

replaced by the singly charged exciton, the trion (X^{1-}). The origin of the strong Coulomb blockade is the nanometer size of the dot which leads to large Coulomb energies [5].

Time correlated single photon counting is used to measure the decay dynamics. We excite the sample non-resonantly with a linearly polarized pulsed laser diode which emits 100 ps pulses at a wavelength of 826 nm. The excitation is absorbed predominantly in the wetting layer. The time response of the system is limited to about 400 ps by the detector, a Si avalanche photodiode, but by convoluting measured decays with the known response of the system, we can determine decay times to an accuracy of about 100 ps. The decay curves are measured in a spectral bandwidth of 0.5 meV, large compared to the Coulomb renormalizations of the emission on charging. The excitation power is kept low enough that we observe no biexciton-related emissions, either in the PL spectra or decay curves.

The crucial experimental result is shown in Fig. 2 within the dynamic range of the experiment, the X^0 exhibits a two-component exponential decay whereas the X^{1-} decay is mono-exponential. The X^{1-} decay time is 0.7 ns, corresponding to the radiative lifetime. In other words, the X^{1-} decay corresponds to radiative decay. The primary X^0 decay has a very similar decay time, 0.5 ns for the dot in Fig. 2, and therefore also corresponds to radiative decay. The interesting question concerns the origin of the secondary X^0 decay. In the experiment on X^0, bright and dark excitons are generated equally as the electron spin is randomized by the electron reservoir during relaxation. When created, a dark exciton has to flip its spin

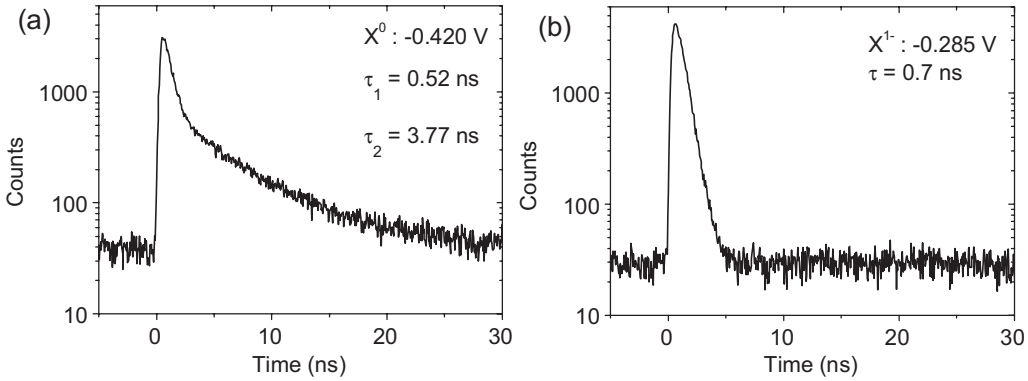

Fig. 2 PL decay curves corresponding to (a) X^0 and (b) X^{1-} measured on the same quantum dot at 5 K. The excitation was a 100 ps pulse at 826 nm. The X^{1-} decay is reproduced well by a single exponential but the X^0 decay requires a second exponential component to achieve a good fit to the data.

© 2005 WILEY-VCH Verlag GmbH & Co. KGaA, Weinheim

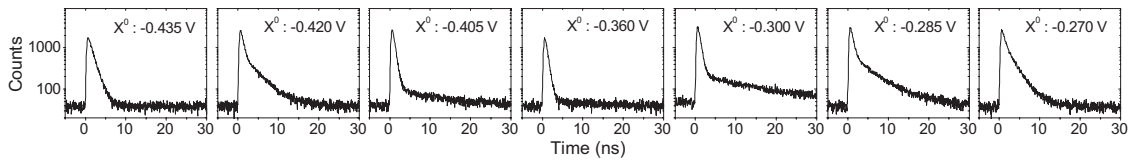

Fig. 3 PL decay curves at various voltages along the X^0 plateau.

in order to become bright and emit a photon. We therefore associate the secondary decay time with the dark exciton dynamics. The mono-exponential decay curves of the X^{1-} reinforce this statement as we can thereby rule out other effects such as minority carrier diffusion.

The secondary decay time, τ_2, varies with voltage as shown in Figs. 3 and 4. X^0 exists between voltages V_1 and V_2. Close to V_1, τ_2 increases from around 1 ns to a maximum of ~20 ns. τ_2 remains at 20 ns before decreasing close to V_2. The behavior is symmetric with respect to $\frac{1}{2}(V_1+V_2)$ suggesting very strongly that the dynamics are related to the Coulomb blockade. However, in the plateau region, the secondary component has a much smaller intensity than the primary and there is also a net loss of signal implying that the decay in this region is dominated by a non-radiative mechanism, in all probability hole tunneling out of the quantum dot.

The decay time τ_2 is dominated by the spin flip time of the dark exciton close to V_1 and close to V_2. The strong voltage dependence rules out an intrinsic spin flip mechanism which would not have a strong voltage dependence. In fact, we can deduce from the present experiment that the intrinsic spin flip time is larger than 20 ns.

The mechanism we propose for the spin flip mechanism is illustrated in Fig. 5. The initial state, the dark exciton, flips its spin by exchanging a spin with an electron close to the Fermi energy in the Fermi sea, forming the bright exciton as final state in this process. The intermediate state has either both electrons in the Fermi sea, dominant near V_1, or both electrons on the quantum dot, dominant near V_2. As we show, this mechanism has the correct voltage dependence and we find quantitative agreement with model calculations.

3 Calculations based on the Anderson Hamiltonian

The starting point of our calculations is the Anderson Hamiltonian which describes the interaction of a localized electron with a Fermi sea of continuum electrons [6]. The true eigenstates are admixtures of localized and continuum states. However, for voltages far enough away from V_1 and V_2, the states are predominantly either quantum dot-like or continuum-like. We therefore assume that the initial state fol-

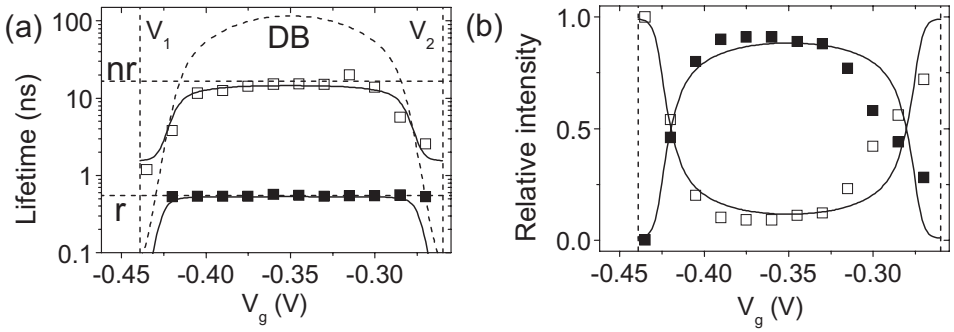

Fig. 4 Lifetimes (a) and relative intensities (b) of the primary and secondary decay components plotted as filled and open symbols, respectively, as a function of V_g. The solid lines are the results of the model calculations taking, with symbols defined in the text, $\Delta = 0.07$ meV, $\gamma_r = 1.8$ ns^{-1}, $\gamma_{nr} = 0.06$ ns^{-1}, $\delta_{BD} = 0.3$ meV and $\Gamma_0 = 50$ μeV. The components γ_r^{-1}, γ_{nr}^{-1} and γ_{DB}^{-1} are shown by the dashed lines.

© 2005 WILEY-VCH Verlag GmbH & Co. KGaA, Weinheim

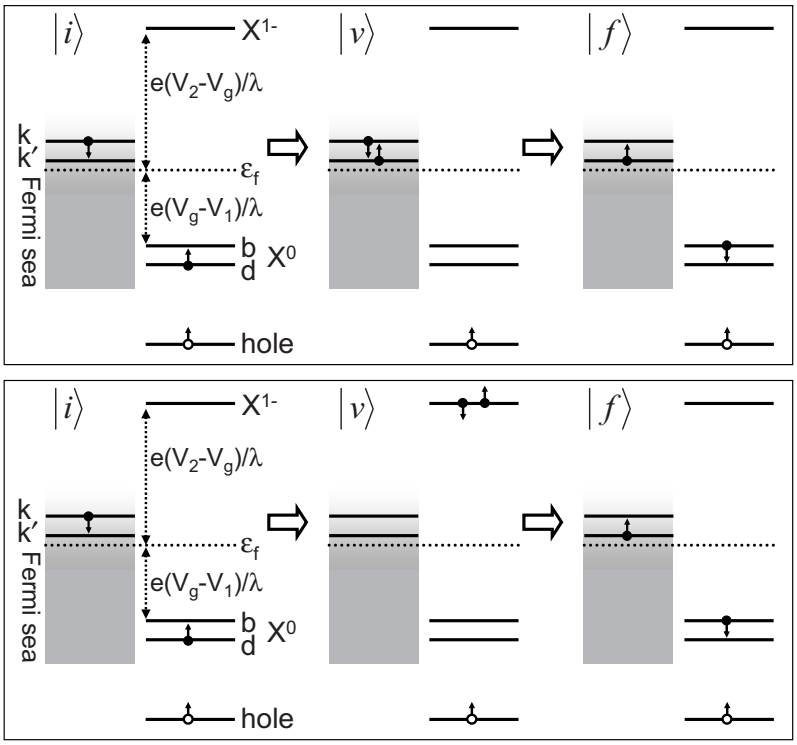

Fig. 5 Schematic representation of the transition of a dark exciton d, initial state $|i\rangle$, to a bright exciton b, final state $|f\rangle$, through two possible intermediate states, $|v\rangle$. The splitting between the dark and bright states is δ_{BD}, exaggerated for clarity. The spin swap process conserves energy such that the participating continuum states must be split by δ_{BD}. The hole spin is assumed to remain constant throughout the process, $+\frac{3}{2}$ in this particular example. Top: both electrons occupy continuum states in the intermediate state; bottom: both electrons occupy the quantum dot in the intermediate state.

lowing photo-excitation is a localized quantum dot state. To calculate the spin-flip rate of a dark to bright exciton, we treat the tunneling term in the Hamiltonian as a perturbation, calculating the rate using Fermi's golden rule. The tunneling term in the Hamiltonian is $\sum_{k,s} V_k(c_{ks}^{\dagger}c_s + c_s^{\dagger}c_{ks})$ where V_k is the tunneling matrix element, $c^{\dagger}$ and c denote creation and annihilation operators, respectively, and s is either spin-$\uparrow$ or spin-$\downarrow$ in a standard notation [6]. In first order, perturbation theory gives a zero result for the spin flip rate as the individual terms in the tunneling Hamiltonian transfer an electron from a localized to a continuum state, or vice versa, maintaining spin. The first non-zero result arises in second order perturbation theory. An alternative approach is to transform the Hamiltonian with the Schrieffer–Wolf canonical transformation which removes terms first order in V. First order perturbation theory can then be used on the transformed Hamiltonian. We follow this approach as it allows a natural connection to be made between the results presented here and the Kondo effect. The transformed Hamiltonian contains several terms to second order in V, but the term responsible for the spin-flip through co-tunneling is

$$\frac{1}{2}\sum_{k,k',s} V_k V_{k'}\left(\frac{1}{\varepsilon_k-\varepsilon_L}+\frac{1}{\varepsilon_{k'}-\varepsilon_L}+\frac{1}{\varepsilon_L+U-\varepsilon_k}+\frac{1}{\varepsilon_L+U-\varepsilon_{k'}}\right)c_{k's}^{\dagger}c_{k-s}c_{-s}^{\dagger}c_s\ , \tag{1}$$

where ε_L is the energy of the localized state, ε_k the energy of the continuum state with wave-vector k, and U is the on-site Coulomb energy. The operators show that this term exchanges a spin between a localized and continuum electron. The amplitude contains two terms. The first two do not involve the on-

© 2005 WILEY-VCH Verlag GmbH & Co. KGaA, Weinheim

site Coulomb interaction and can be associated with the process shown in the upper part of Fig. 5 where the intermediate state has an empty localized state. Conversely, the second two terms do involve the on-site Coulomb interaction and can be associated with the process shown in the lower part of Fig. 5 where the intermediate state has a doubly occupied localized state. This particular operator in the transformed Hamiltonian ultimately leads to the Kondo effect when the tunneling is highly coherent.

The energy separations in the denominators in Eq. (1) are determined by the electrostatics of the device. Converting the applied voltage into an electrostatic energy with the lever arm model [5], the singly-occupied quantum dot level lies $e(V_g - V_1)/\lambda$ beneath the Fermi energy, and the doubly-occupied quantum dot level lies $e(V_2 - V_g)/\lambda$ above the Fermi energy (Fig. 5), where λ is the lever arm, 7 for this particular device.

The individual terms in Eq. (1) involve two continuum states with wave vector k and k'. They are separated in energy by the splitting between the dark and bright states as demanded by energy conservation as the hole spin is constant. Clearly, the total rate is determined by summing over all the continuum states, taking into account the occupation factors. We do this in the standard way with the density of states and Fermi–Dirac function. The product of two Fermi–Dirac functions, $f(\varepsilon)$ and $[1 - f(\varepsilon - \delta_{BD})]$, where ε is the energy, and δ_{BD} the splitting between the dark and bright states, with the Fermi energy ε_f defined to lie at zero energy, implies that only states within a few $k_B T$ of the Fermi energy contribute to the integral. This in turn means that over this range we can neglect the k-dependence of V_k and also any energy dependence of the density of continuum states. The denominators in Eq. (1) result in singularities and potentially unphysical results. The singularities will disappear in a more complete treatment which includes the dephasing of the initial and final states. In our approximate account, we introduce the dephasing of the initial and final states through an imaginary term, motivated by the self energy. We finally arrive at the following result for γ_{DB}, the transition rate from the dark to bright exciton,

$$\gamma_{DB} = \frac{\Delta^2}{h} \int_{\varepsilon} \left| \frac{1}{\varepsilon + e(V_g - V_1)/\lambda + \frac{i}{2}\Gamma} + \frac{1}{e(V_2 - V_g)/\lambda - \varepsilon + \frac{i}{2}\Gamma} \right|^2 f(\varepsilon)\,[1 - f(\varepsilon - \delta_{BD})]\,\mathrm{d}\varepsilon \,. \tag{2}$$

Γ is the energy broadening of the exciton states and Δ is a tunnel energy, $\Delta = 2\pi |V|^2 \, g(\varepsilon_f)$, $g(\varepsilon)$ being the density of states. We describe the energy broadening Γ by reference to the experiment. There is a voltage-independent term Γ_0 which arises from scattering with optically-excited carriers and phonons and there is also a tunneling related term which depends on voltage,

$$\Gamma = \Gamma_0 + 2\Delta[f(e(V_g - V_1)/\lambda) + f(e(V_2 - V_g)/\lambda)] \,. \tag{3}$$

Strictly of course, the spin-flip process described by Eq. (2) contributes to Γ but we find that in the voltage regime where the model is valid, the spin-flip process makes a very minor contribution to the linewidth.

A number of comments can be made from the result for γ_{DB}. First, the result for γ_{DB} depends quadratically on the tunnel energy, exactly as expected for a two-particle co-tunneling process. Secondly, γ_{DB} has a strong voltage dependence through the electrostatic energies, the largest energies in the problem. In fact the theoretical result is symmetric around $\frac{1}{2}(V_1 + V_2)$, exactly as in the experiment. Thirdly, γ_{DB} has a temperature dependence through the Fermi–Dirac functions. γ_{DB} increases as the temperature increases through a softening of the Fermi–Dirac functions. Conversely, when $T \ll \delta_{BD}$, as $T \to 0$, $\gamma_{DB} \to 0$ as in this case there is little overlap between $f(\varepsilon)$ and $[1 - f(\varepsilon - \delta_{BD})]$. Fourthly, the same mechanism, electron spin-swap with the Fermi sea, can convert a bright into a dark exciton and a similar result for γ_{BD} can be derived. In this case, the product of occupation factors becomes $f(\varepsilon - \delta_{BD})\,[1 - f(\varepsilon)]$, resulting in $\gamma_{BD} \simeq \mathrm{e}^{\delta_{BD}/k_B T} \gamma_{DB}$. In our experiment at 5 K, $\gamma_{BD} \simeq \gamma_{DB}$ but at lower temperature $\gamma_{BD} > \gamma_{DB}$. As a final remark we note that γ_{DB} depends on the product of $|V|^2$ and $g(\varepsilon_f)$ and not on either term individually, facilitating a detailed comparison with the experiment.

 © 2005 WILEY-VCH Verlag GmbH & Co. KGaA, Weinheim

A significant strength of our experiment is that we can determine the parameters required to calculate γ_{DB}, equivalently γ_{BD}, from the PL spectra. δ_{BD} can be measured even at zero magnetic field by measuring the PL from more highly charged excitons for which the "dark" states become bright [7]. We find that $\delta_{BD} = 0.3$ meV for the dot in Fig. 4. Δ can be measured through the X^{1-} emission for voltages just larger than V_2. We have recently demonstrated that at this voltage the single electron in the final state tunnels out after recombination [8] such that the PL FWHM is 2Δ. This gives $\Delta = 0.07$ meV for the dot in Fig. 4. The corresponding tunneling time is $\tau_t = \Delta/\hbar = 9$ ps, considerably less than the radiative recombination time. We can also back up these measurements of the tunneling time with estimates based on the result in [9] for 0D–3D tunneling. For the dot in Fig. 4, we estimate the electron ionization energy to be 95 meV from the experimental Coulomb blockade (Fig. 1), and the tunnel barrier thickness is known to be 25 nm from the growth. The tunneling time depends exponentially on these parameters [9]. The tunneling time depends relatively weakly on the prefactor to the exponential which contains the vertical confinement, the height and the electron effective mass which we estimate as 220 meV, 3 nm (the approximate z-direction wave function extent of our nanostructures [10]) and $0.07m_0$ (the mass determined from spectroscopy in a magnetic field [11]), respectively. The result is 12 ps, proving that the experimental value of 9 ps is very reasonable for our structure. Γ_0 is determined by the spectral linewidth of the X^0 exciton around $V_g \simeq \frac{1}{2}(V_1 + V_2)$. The linewidth is smaller than the spectral resolution in this particular experiment making it difficult to determine Γ_0 accurately. We estimate $\Gamma_0 \simeq 50$ μeV. We note however that the results for γ_{DB} are only weakly dependent on Γ_0 and within the error for Γ_0 they change only by a few %. The PL spectra show that the X^0 linewidth is larger for voltages close to V_1 and V_2 than it is for voltages close to $\frac{1}{2}(V_1 + V_2)$, and this increase is compatible with broadening resulting from single electron tunneling, exactly the content of Eq. (3).

The decay curves depend on the radiative rate γ_r, the spin-flip rates γ_{DB}, γ_{BD} and non-radiative decay through the hole tunneling rate γ_{nr}. To calculate the primary and secondary lifetimes and intensities we use a rate equation model, considering 3 levels, the vacuum state, the dark state with occupation n_D and the bright state with occupation n_B, as illustrated in Fig. 6. The rate equations are

$$\begin{aligned} \frac{dn_B}{dt} &= -n_B(\gamma_{BD} + \gamma_{nr} + \gamma_r) + n_D\gamma_{DB}\,, \\ \frac{dn_D}{dt} &= -n_D(\gamma_{DB} + \gamma_{nr}) + n_B\gamma_{BD}\,. \end{aligned} \tag{4}$$

The solutions to the rate equations yield a bi-exponential decay, exactly as in the experiment, $n_B(t) = a_1\, e^{-\gamma_1 t} + a_2\, e^{-\gamma_2 t}$ with

$$\gamma_{1,2} = \tfrac{1}{2}(\gamma_r + 2\gamma_{nr} + \gamma_{DB} + \gamma_{BD}) \pm \tfrac{1}{2}\sqrt{\gamma_r^2 + 2\gamma_r(\gamma_{BD} - \gamma_{DB}) + (\gamma_{DB} + \gamma_{BD})^2}\,,$$

$$a_{1,2} = \pm n_B(0)\,\frac{\gamma_r + \gamma_{BD} + \gamma_{nr} - \gamma_{2(1)}}{\gamma_1 - \gamma_2} \mp n_D(0)\,\frac{\gamma_{DB}}{\gamma_1 - \gamma_2}\,. \tag{5}$$

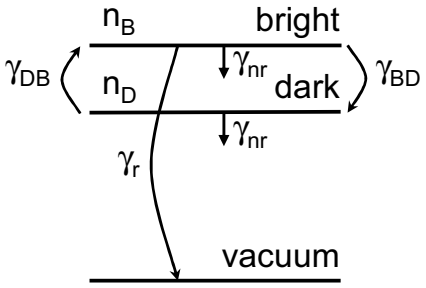

Fig. 6 Three levels taken into account in the rate equations: the vacuum state, the dark exciton and bright exciton. The bright and dark states are connected by a spin-flip process; the bright exciton can decay radiatively; and both dark and bright excitons can decay non-radiatively by hole tunneling out of the dot.

© 2005 WILEY-VCH Verlag GmbH & Co. KGaA, Weinheim

These equations yield intuitive results in the limit $\gamma_r \gg \gamma_{BD}, \gamma_{DB}$ namely $\gamma_1 \simeq \gamma_r + \gamma_{BD} + \gamma_{nr}$ and $\gamma_2 \simeq \gamma_{DB} + \gamma_{nr}$. In other cases however, the relationship of the measured rates $\gamma_{1,2}$ to the radiative, non-radiative and spin flip rates is more complicated. We assume that the initial state populations of dark and bright excitons are equal, $n_B(0) = n_D(0)$. This is a good approximation because, first, the highly non-geminate capture processes following highly non-resonant excitation in our device imply a random exciton spin, and second, our own results and also those of other groups [12] show that thermalization of the exciton spin takes much longer than a ns.

Figure 4 shows the final result of the calculation. The model accounts extremely well for the bias dependence of the lifetimes and relative intensities. The calculation makes it clear that we can tune γ_{DB} to be both larger and much smaller than γ_r. The dependence on tunneling energy and temperature in Eq. (2) has also been experimentally verified [13].

4 Conclusions and outlook

The exciton decay dynamics of a single self-assembled quantum dot clearly reveal components due to radiative recombination of the bright exciton and a spin flip of the dark exciton. We demonstrate that the most important spin flip mechanism in our device involves a spin flip with a Fermi sea, a reservoir of charge interacting with the quantum dot through a tunneling interaction. This imparts a strong voltage dependence to the spin flip time. This is a significant result: the exciton spin flip time can be manipulated to be smaller or much larger than the radiative recombination time simply with a small dc voltage. We demonstrate quantitative agreement with our results with a model based on the Anderson Hamiltonian, enabling us to interpret the spin flip mechanism as a Kondo-like interaction. Our results therefore suggest that in a more coherent process, involving a smaller dark-bright exciton splitting, a lower temperature and perhaps a higher electron mobility in the Fermi sea, it will be possible to observe an optical Kondo effect.

Acknowledgements This work was funded by EPSRC (UK), Ohio University and the Volkswagen and Alexander von Humboldt Foundations. JMS was supported by the Scottish Executive and the Royal Society of Edinburgh. We would like to thank Ian Galbraith for helpful discussions.

References

[1] M. Bayer et al., Phys. Rev. B **65**, 195315 (2002).
[2] A. Högele, S. Seidl, M. Kroner, K. Karrai, R. J. Warburton, B. D. Gerardot, and P. M. Petroff, Phys. Rev. Lett. **93**, 217401 (2004).
[3] J. J. Finley, D. J. Mowbray, M. S. Skolnick, A. D. Ashmore, C. Baker, A. F. G. Monte, and M. Hopkinson, Phys. Rev. B **66**, 153316 (2002).
[4] A. I. Tartakovskii, J. Cahill, M. N. Makhonin, D. M. Whittaker, J.-P. R. Wells, A. M. Fox, D. J. Mowbray, M. S. Skolnick, K. M. Groom, M. J. Steer, and M. Hopkinson, Phys. Rev. Lett. **93**, 057401 (2005).
[5] R. J. Warburton, B. T. Miller, C. S. Dürr, C. Bödefeld, K. Karrai, J. P. Kotthaus, G. Medeiros-Ribeiro, P. M. Petroff, and S. Huant, Phys. Rev. B **58**, 16221 (1998).
[6] G. D. Mahan, Many-Particle Physics, 3rd edition (Plenum Press, New York, 2000).
[7] B. Urbaszek, R. J. Warburton, K. Karrai, B. D. Gerardot, P. M. Petroff, and J. M. Garcia, Phys. Rev. Lett. **90**, 247403 (2003).
[8] S. Seidl, M. Kroner, P. A. Dalgarno, J. M. Smith, A. Högele, M. Ediger, B. D. Gerardot, J. M. Garcia, P. M. Petroff, K. Karrai, and R. J. Warburton, accepted for Phys. Rev. B (2005).
[9] J. M. Villas-Bôas, S. E. Ulloa, and A. O. Govorov, Phys. Rev. Lett. **94**, 057404 (2005).
[10] R. J. Warburton, C. Schulhauser, D. Haft, C. Schäflein, K. Karrai, J. M. Garcia, W. Schoenfeld, and P. M. Petroff, Phys. Rev. B **65**, 113303 (2002).
[11] K. Karrai, R. J. Warburton, C. Schulhauser, A. Högele, B. Urbaszek, E. J. McGhee, A. O. Govorov, J. M. Garcia, B. D. Gerardot, and P. M. Petroff, Nature **427**, 135 (2004).
[12] M. Paillard, X. Marie, P. Renucci, T. Amand, A. Jbeli, and J. M. Gérard, Phys. Rev. Lett. **86**, 1634 (2001).
[13] J. M. Smith, P. A. Dalgarno, R. J. Warburton, A. O. Govorov, K. Karrai, B. D. Gerardot, and P. M. Petroff, Phys. Rev. Lett. **94**, 197402 (2005).

 © 2005 WILEY-VCH Verlag GmbH & Co. KGaA, Weinheim